Behavior of Steel Joist Girder Structures with PR Column Bases

UKSUN KIM, ROBERTO T. LEON, AND THEODORE V. GALAMBOS

Single story, joist girder buildings (Figure 1) are used extensively as work areas for industry, for light manufacturing, storage, retail, or other commercial uses. There are thousands of these low-rise facilities in the United States, and as new seismic risk maps extend the seismic design requirements to larger areas, the development of rational seismic design procedures for this type of structure is a pressing need. Changes in seismic design towards performance-based procedures mean that even industrial-type structures will be required to demonstrate some ductility and incorporate at least some basic seismic detailing to avoid large economic losses during small to moderate earthquakes.

From the seismic design standpoint, joist girder frames are unique in that: (1) the columns are very long and carry relatively light axial loads, resulting in very flexible structures; (2) their design is controlled by drift criteria more liberal than for traditional structures (drift limits are often in the range of $H/100$ to $H/250$ as opposed to $H/400$ for traditional buildings under the design wind load, where H is the height of the structure); (3) most joist girder frames are designed assuming rigid connections at the girder-to-column joint and pinned or rigid connections at the base without specific requirements for these assumptions to be checked; and (4) for this class of structures, there are no specific analysis and design recommendations readily available for seismic design. This paper reports on a combined analytical/experimental investigation aimed at: (1) assessing the frame behavior of joist girder frames with different column base fixities (pinned and partially restrained); (2) evaluating the stiffness and strength of column bases by means of both experimental and analytical approaches; and (3) developing seismic design procedures that account for the real column base conditions. A companion paper (Kim, Leon, and Galambos, 2007) discusses in detail other design aspects and provides an example design for this type of structure.

Uksun Kim is assistant professor, department of civil and environmental engineering, California State University, Fullerton, CA.

Roberto T. Leon is professor, school of civil and environmental engineering, Georgia Institute of Technology, Atlanta, GA.

Theodore V. Galambos is professor emeritus, department of civil engineering, University of Minnesota, Minneapolis, MN.

BACKGROUND

Joist girder building design is typically governed by drift under wind loads. The allowable drift is controlled by the flexibility of the exterior wall system, which can range from very flexible (metal sheathing) to stiff (precast concrete). While its flexibility is used to select the drift criterion, the effect of the wall system is usually not included in the analysis, so the resulting analytical model is a very flexible one when checked against current seismic drift criteria (ASCE, 2005; AISC, 2005). In addition, the analysis of these structures is carried out using the conventional simplification of assuming either rigid or pinned connections, and no specific checks are conducted to assess deformation capacity beyond the elastic limit. These assumptions need to be reconsidered

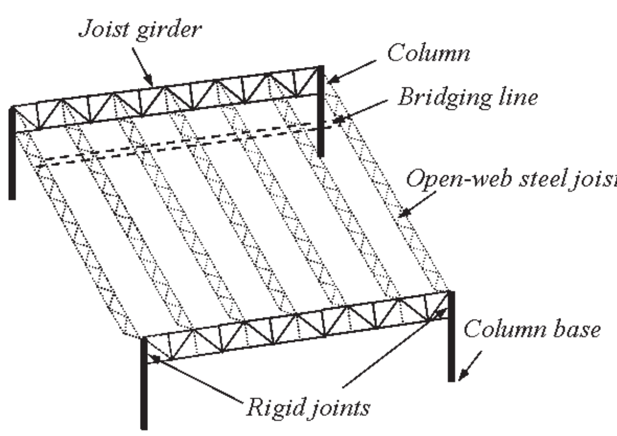

Fig. 1. One-bay, one-story steel joist girder structure.

for seismic design, insofar as they may not necessarily be conservative. Moreover, little guidance is currently provided to the designer by codes on how to detail a rigid girder-to-column connection for these structures or how to obtain true pinned behavior at the column base. This paper addresses how to design and detail a column base and its effect on the behavior of joist girder structures. The design of the girder-to-column connection is assumed to provide sufficient moment resistance and rotational ductility to trigger a weak column-strong beam mechanism (Kim et al., 2007).

Column bases in joist girder frames generally consist of two or four anchor rods (Figures 2 and 3) embedded in a concrete foundation. These column bases are assumed to transfer only the axial and shear forces to the foundation, as their moment capacity and stiffness are considered to be small. Two reasons are often given to justify this approach. First, ignoring the moment capacity and stiffness of the column bases is assumed to be conservative. Second, there are no simple procedures to calculate the strength and stiffness in column bases, and most design specifications pay little attention to them. There are at least two strong motivations for not accepting this reasoning. First, for structures in seismic regions, a significant moment may be induced at the column bases due to the inertial loads, resulting in a significant redistribution of forces and potential overloading of critical members. Second, the latest OSHA regulations related to steel erection safety (OSHA, 2001) require at least four anchor rods, resulting in a stiffer and stronger column base. Existing studies indicate that the introduction of a partially restrained (hereafter, PR) model for the column bases may result in a noticeable effect on the column stability and overall frame behavior (Picard and Beaulieu, 1985; Picard, Beaulieu, and Pérusse, 1987; Stojadinović, Spacone, Goel, and Kwon, 1998).

Simplified analytical models that span the entire range from flexible to rigid base plates have recently become available through the use of the so-called 'component method' (Wald and Jaspart, 1998). In this European methodology, the base plate connection is broken down into a series of components (anchor rods in tension and shear, plate in bending, column flanges in tension and compression, etc.) and the base plate response is determined from a model that incorporates all the relevant yielding and failure modes in the form of linear springs. While this model has been extensively tested against typical European base plate configurations, there has been comparatively little research on United States detailing practice or on full-scale frame specimens to ascertain the effects of low to moderate amounts of base fixity. The research described herein began with the design of several trial frames for areas of different seismicity. From those prototypes, a single-bay section was selected for testing. The experimental results were then used, along with the component method, to develop simple column base moment-rotation models. Finally a complete seismic design procedure was proposed.

DESIGN OF EXAMPLE FRAMES

As a first step in this study, trial joist girder frames were designed for three locations (Los Angeles, Salt Lake City, and Boston) representing different ranges of wind, snow and earthquake loads. Parts of several design codes and specifications were used as the basis for design (ASCE, 2005; AISC, 2001; ICC, 2000; SJI, 2002). The design of these

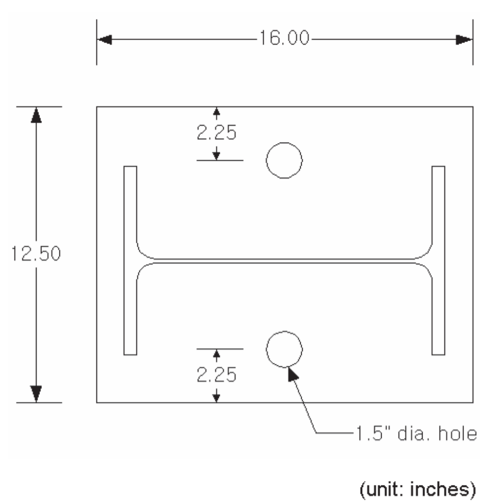

Fig. 2. Column base with two anchor rods.

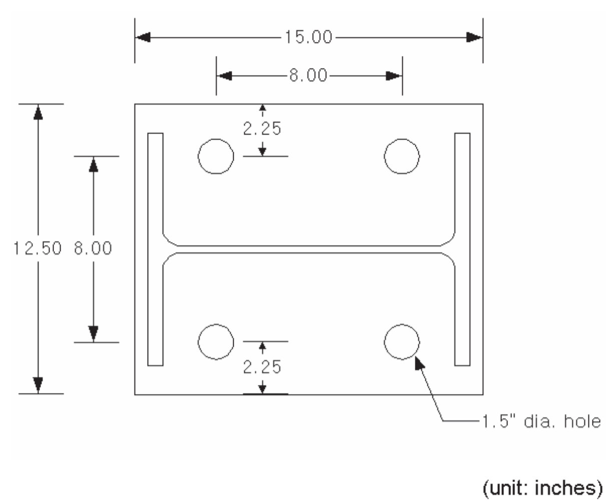

Fig. 3. Column base with four anchor rods.

Table 1. Description of Two Prototype Frames			
	Full-Scale Test Model	Practical Construction Model	
General	One-bay, one-story Height: 5.5 m (18 ft) Span: 12.2 m (40 ft) Location: Boston, MA	Three-bay, one-story Height: 9.1 m (30 ft) Span: 12.2 m (40 ft) per bay Location: Los Angeles, CA	
Column base	Two anchor rods (Figure 2)	Four anchor rods inside the flanges (Figure 3)	
Joist	26K7 [a]	24K4 [a]	
Joist Girder	40G8N11K (40G8N11K)	40G8N8K (40G8N8K)	
Column	W360×64 (W14×43)	Interior	W360×91 (W14×61)

[a] The member designations are based on SJI specifications (SJI, 2002).

structures was generally governed by drift due to wind, with typical values of allowable drift taken as $H/100$ based on assuming a flexible curtain wall system. Two example frames were selected for these trial designs as shown in Table 1. The first was a one-story, one-bay subassemblage that was used as the prototype for a full-scale cyclic test. The second was a one-story, three-bay frame that was used for the analytical studies and which took realistic construction constraints into account. The analyses were performed using Computers and Structures (1998), and Hibbit, Karlsson, and Sorensen (1998), and the designs were made with the aid of MathCad spreadsheets (Mathsoft, 2000). The details for the column bases for the two frames can be seen in Figures 2 and 3. The detail presented in Figure 2 is no longer permitted due to the latest OSHA requirements, but this detail was used in the full-scale test and its moment-rotation behavior quantified.

FULL-SCALE CYCLIC TEST

The dimensions for the test frame are summarized in Table 1 and the test setup can be seen in Figure 4. Figure 5 shows an overview of the full-scale test. The specimen consisted of two parallel frames braced against each other at the ends and connected by open-web steel joists and a metal roof deck. Thus the specimen captures all of the relevant behavioral modes for this type of structure, including the nonlinear performance of both the joist girder-to-column moment connections and the column bases. Seven large concrete blocks (about 44.5 kN or 10 kips each) were hung on alternating panel points of the joist girders to simulate the gravity load and to allow it to be maintained through large cyclic displacements.

The structure was instrumented as seen in Figure 6. The locations and number of the column strain gages were selected in order to obtain a good estimate of the column and

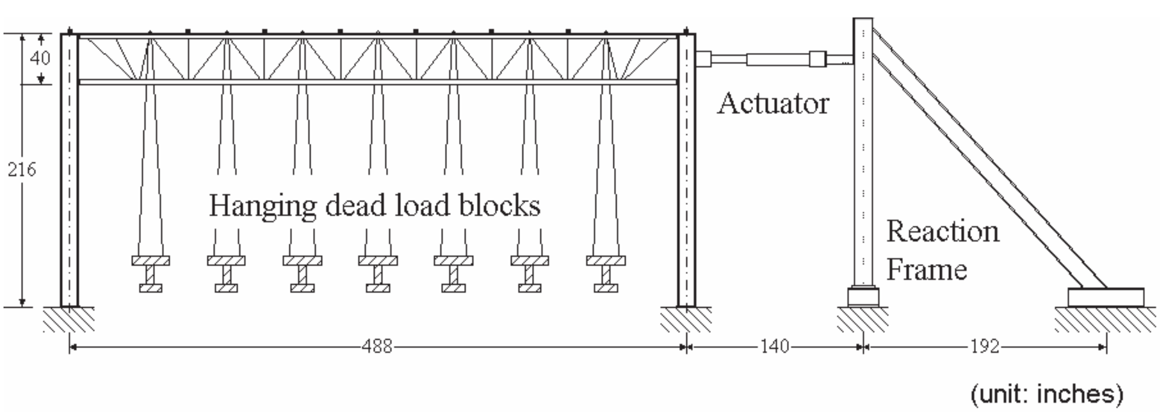

Fig. 4. Test setup.

joist girder axial and flexural strains after yielding. The gages on the columns were located at a distance of $2d$ (d = depth of column member) from both the bottom chord connection and the base plate to ensure measurements in an area with a smooth strain distribution and to minimize any localized effects due to welding of the connection or base plates.

For the cyclic test, the concrete blocks simulated 100% of the dead load and 20% of the roof live load plus snow load. This corresponds roughly to 1.2 times the conventional seismic mass assumed in design. The structure was loaded in displacement control to obtain the interstory drifts prescribed by the SAC protocol (Figure 7) (SAC, 1997). The lateral load vs. displacement curve is shown in Figure 8, while the moment-rotation curve obtained for the column base at the right side of the front frame is shown in Figure 9, and the moment-rotation behavior of the joist girder-to-column connection is shown in Figure 10. From these figures, the average rotational stiffness of the connection between the joist girder and the columns, K_{connc}, was about 6.2×10^5 kN-m/radian (5.5×10^6 kip-in./radian) while that of the column base, K_{base}, in its initial elastic phase was about 2.6×10^3 kN-m/radian (2.3×10^4 kip-in./radian). Based on comparisons with established limits for connections stiffness (AISC, 2001), the connection at the top can be assumed to be fully restrained (FR) or rigid, while that at the bottom is a weak PR (semi-rigid) one.

The behavior of the frames was linear until the interstory drift reached 2% [110 mm (4.32 in.)], at which point the columns began to hinge immediately below the connection to the bottom chord of the joist girder. Full plastification of the cross-section in these areas was observed at 3% interstory drift, and the test was stopped shortly thereafter due to the out-of-plane displacement of the frames, which were braced against each other but not to any external point. When all four column tops formed plastic hinges, the lateral restraint on the columns decreased and the initiation of an inelastic flexural-torsional buckling global failure was observed. The

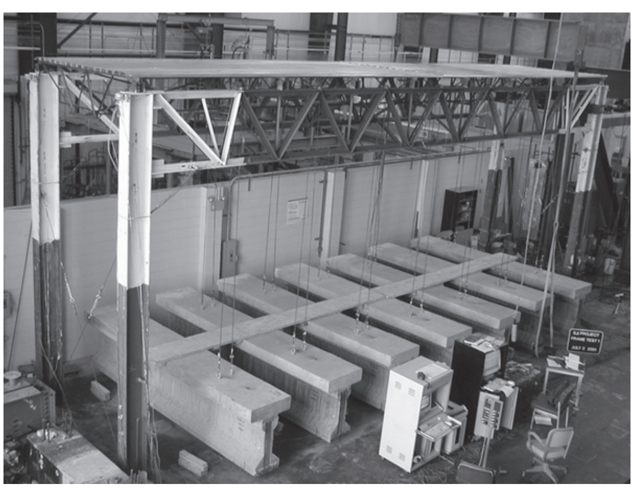

Fig. 5. Overview of test setup.

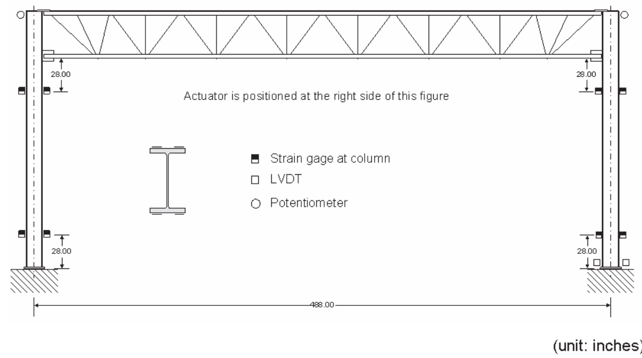

Fig. 6. Sensor locations.

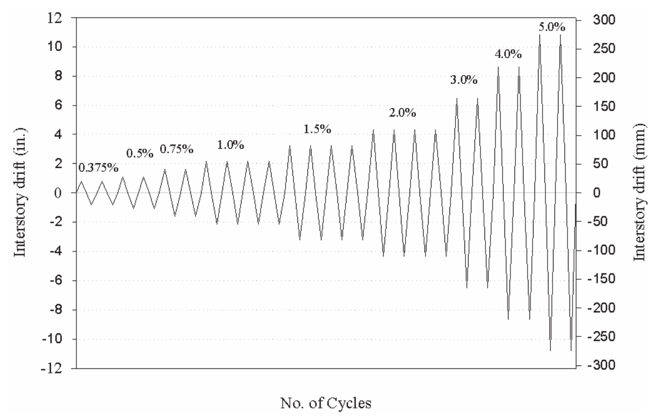

Fig. 7. Lateral load history.

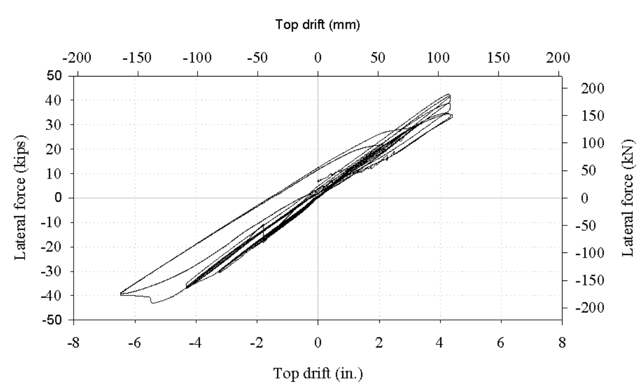

Fig. 8. Load-displacement curve of the test frame.

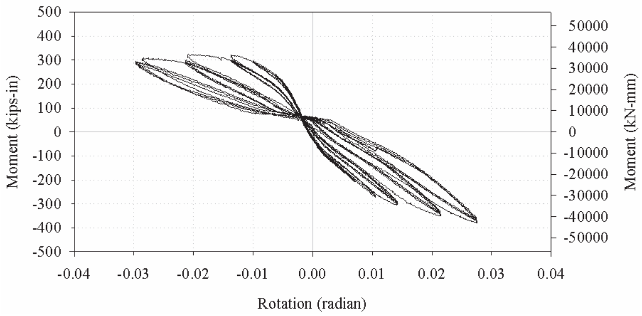

Fig. 9. Moment-rotation curve of the column base.

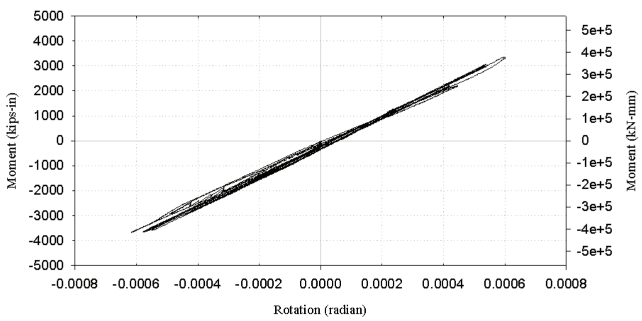

Fig. 10. Moment-rotation curve of the joist girder-to-column connection.

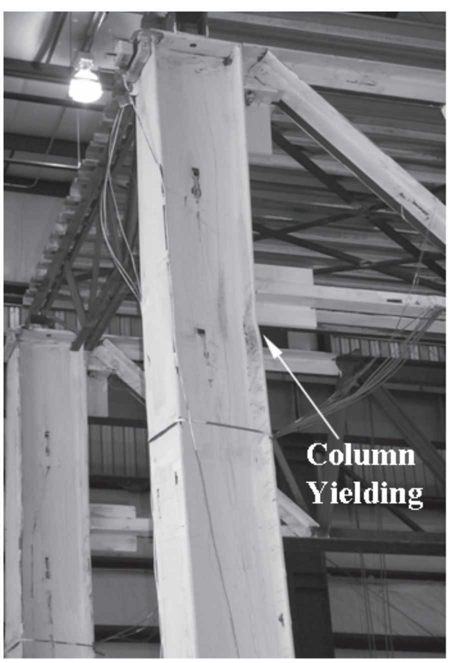

Fig. 11. Plastic hinge formation at the column.

plastic hinge formation at the column is as shown in Figure 11. Figure 12 shows the uplift of the column base during the cyclic test.

ANALYTICAL MODEL FOR PR BASE AND CONNECTIONS

From the connection classification criteria available in the literature (Leon, 1994; AISC, 2001), the column bases can be treated as PR base connections and the joist girder-to-column connections can be treated as rigid connections. Based on the COST C1 report (European Commission, 1999), the stiffness and resistance of the column base can be calculated analytically by the component method, which was initially introduced for beam-to-column joints in the revised Annex J of Eurocode 3 (CEN, 1998). The component method is comprised of two main steps. In the first step, the stiffness, strength and ductility of each component are calculated with due consideration to all pertinent yield and failure mechanisms. The characteristics of each component are generally determined from tests on individual components with carefully monitored boundary conditions. The main components for a column base are as shown in Figure 13. In these components, the main contributions to the stiffness come from (a) the concrete block, (b) the steel T-stub, and (c) the steel anchor rods. In the second step, the stiffness, strength and deformation capacity of the column base as a whole are determined from the assembly of all the components. In the elastic range, where stiffness is the main parameter, the stiffness coefficients of the three major components are given by Equations 1 through 3:

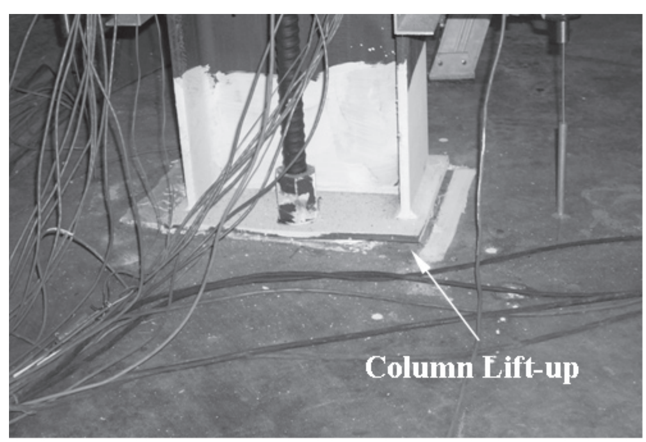

Fig. 12. Uplift of the column base.

Table 2. Comparison Between Rotational Stiffnesses			
Test (refer to Figure 9)		**Component Method**	
Rotational Stiffness	**Moment Capacity**	**Rotational Stiffness**	**Moment Capacity**
2,637 kN-m/rad (23,333 kip-in./rad)	39.6 kN-m (350 kip-in.)	2,772 kN-m (24,520 kip-in./rad) (5.1% ↑)	40.8 kN-m (361 kip-in.) (3.0% ↑)

Stiffness coefficient of concrete component, k_c

$$k_c = \frac{E_c\sqrt{a_{eqel}L}}{1.275E_s} \tag{1}$$

Stiffness coefficient of the plate, k_p

$$k_p = \frac{0.85 l_{eff} t_p^{\,3}}{m^3} \tag{2}$$

Stiffness coefficient of the anchor rod, k_b

$$k_b = 1.6\frac{A_s}{L_b} \tag{3}$$

where

E_c = modulus of elasticity for concrete
a_{eqel} = equivalent width of the T-stub
L = length of the T-stub
E_s = modulus of elasticity for steel
l_{eff} = effective length
t_p = plate thickness
m = geometrical characteristic for the base plate
A_s = anchor rod area
L_b = anchor rod length (Figure 14)

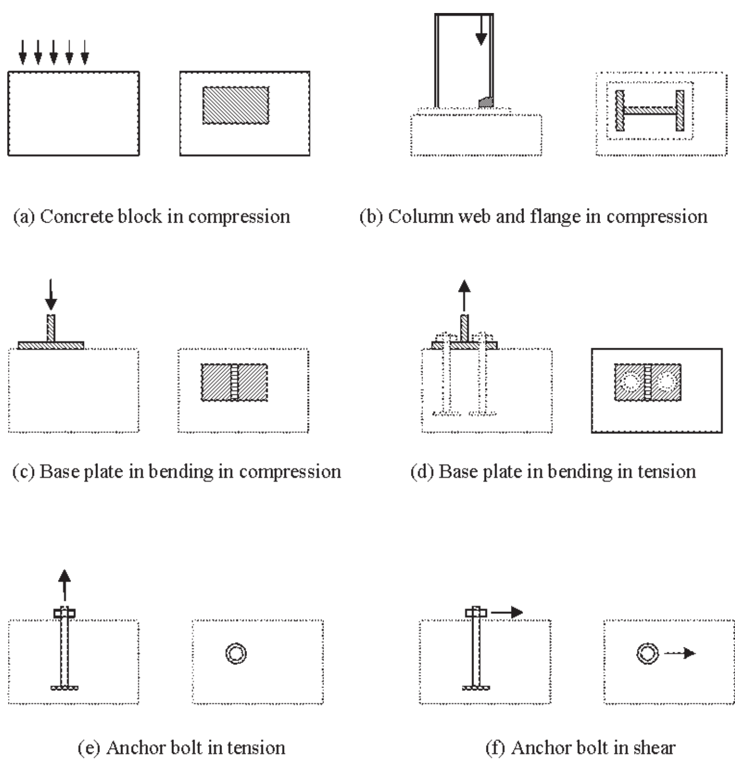

Fig. 13. Components for column base (Wald and Jaspart, 1998).

Equations 1 through 3 can be used in both SI units and U.S. customary units. The assembled elastic stiffness of the column base is given by

$$S_j = \frac{E_s z}{\dfrac{1}{k_c} + \dfrac{1}{k_p} + \dfrac{1}{k_b}} \tag{4}$$

where

z = length of the lever arm as shown in Figure 14

Comparisons between the predictions from the component method and the test results (Table 2) show an excellent agreement. A bilinear model, based on the results from the full-scale test and component method, was developed for the two-anchor rod base plate used in the full-scale test, and for the four-anchor rod base plates for the columns of a three-bay joist girder frame (Figure 15). Though the test results showed that the secondary rotational stiffness was about 25% of the initial rotational stiffness for the two anchor rod configuration, in the model for the four anchor rod configuration, the secondary rotational stiffness was assumed as only 10% of the initial stiffness based on typical assumptions for strain hardening of steel.

FRAME RESPONSE OF PINNED AND PR BASES

The effect of column base fixity on the overall behavior of the one bay and three bay frames was investigated using primarily eigenvalue and pushover analyses. For these types of structures, almost 99% of modal participation mass is related to the first sway mode as shown in Figure 16. Table 3 shows a comparison of the natural periods, up to the 5th mode for the pinned and PR column base cases. The natural period for

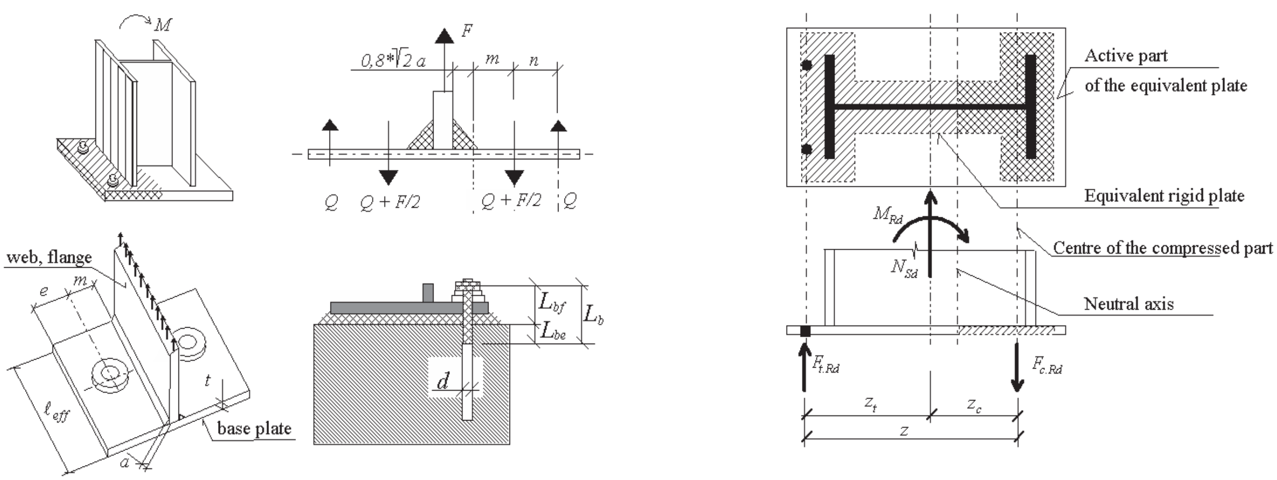

Fig. 14. Definition of dimensions for column base (European Commission, 1999).

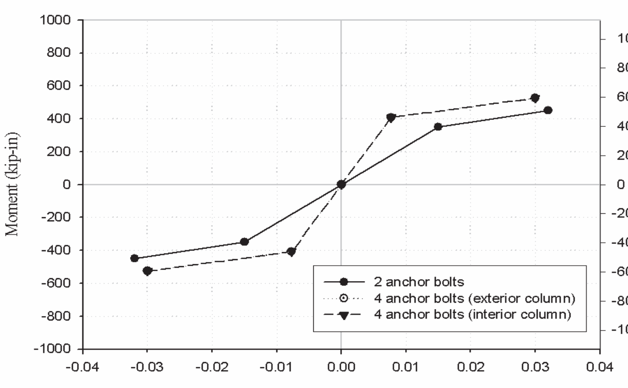

Rotational Stiffness	2 anchor bolts	4 anchor bolts exterior column	4 anchor bolts interior column
Initial	2637 kN-m/rad (23333 kip-in/rad)	5972 kN-m/rad (52850 kip-in/rad)	5994 kN-m/rad (53040 kip-in/rad)
Secondary	665 kN-m/rad (5882 kip-in/rad)	597 kN-m/rad (5285 kip-in/rad)	599 kN-m/rad (5304 kip-in/rad)

Fig. 15. Bilinear models for the different column bases.

Table 3. Natural Periods for the Pinned and PR Column Base				
	Mode	Pinned	PR	Difference %
		Period, s	Period, s	
One-Bay Frame	1	0.739	0.655	–12.2
	2	0.218	0.218	0.0
	3	0.079	0.079	0.0
	4	0.051	0.051	0.0
	5	0.040	0.040	0.0
Three-Bay Frame	1	1.450	1.116	–22.8
	2	0.207	0.206	–0.5
	3	0.177	0.176	–0.6
	4	0.155	0.155	0.0
	5	0.085	0.085	0.0

• For PR base, rotation stiffness of one-bay frame is 2637 kN-m/rad (23,333 kip-in./rad).
• For PR base, rotation stiffness of external column base is 5972 kN-m/rad (52,850 kip-in./rad).
• For PR base, rotation stiffness of interior column base is 5994 kN-m/rad (53,040 kip-in./rad).

mode 1 shows a significant difference due to the effect of column base restraint, but there is little, if any, difference for all other modes. The latter modes, however, have little significance in this type of structure. For the three-bay frame, the natural period is reduced by 22% due to column base restraint. This difference may result in a significant increase of induced base shear and consequent changes in frame response under some seismic excitations.

For the investigation of overall nonlinear frame behavior under lateral loads, nonlinear pushover analyses were performed. Figure 17 contains the base shear-displacement curves for the four column base conditions examined: pinned, linear PR, bilinear PR and fixed for a one-bay frame. Comparison with the full-scale test results is also shown. The practical drift limit (H/100) is 54.9 mm (2.16 in.). There are significant behavioral differences between the frames with different column base fixities. Figure 18 is

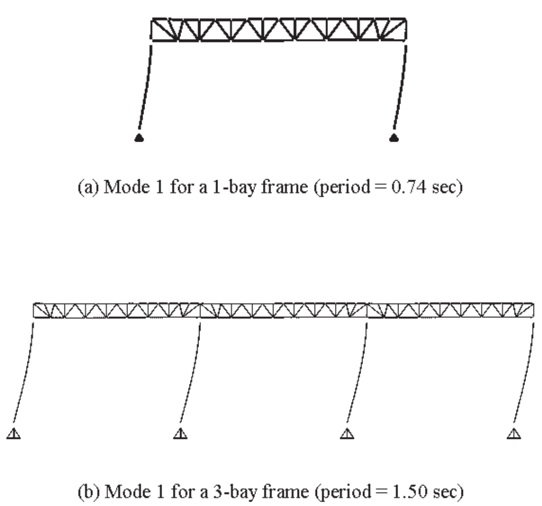

Fig. 16. Mode shapes and natural periods.

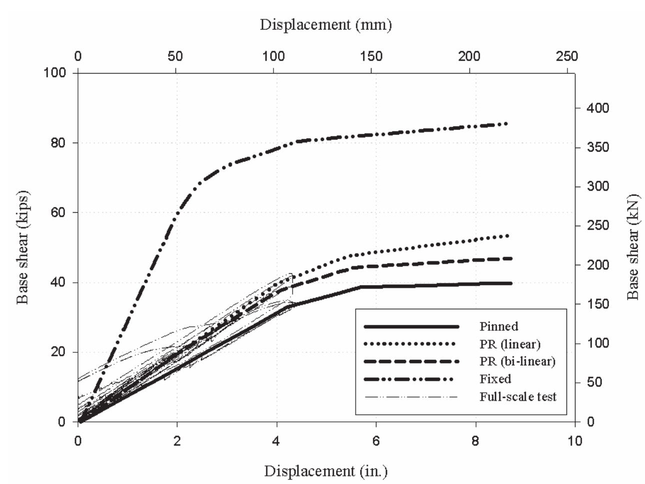

Fig. 17. Pushover curves for column base fixity (one-bay frame).

Table 4. Moment for the Column Members of the One-Bay Frame				
Member	Location	Moment in kN-m (kip-in.)		$\|M_{bse} / M_{top}\|$ for PR Base
		Pinned	Bilinear PR	
Left Column	Top	–413 (–3,656)	–414 (–3,668)	0.169
	Base	0 (0)	70 (621)	
Right Column	Top	–423 (–3,745)	–425 (–3,757)	0.162
	Base	0 (0)	69 (609)	

a magnified view for the initial part of the pushover results. From the comparison with the experimental results, it can be seen that the most realistic frame behavior is given by considering partial column base fixity. From the pushover analyses, the frame with bilinear PR column bases requires 18% additional force as compared to the force required for the frame with pinned column bases. This translates into a significant extra force into the joist girder members, and thus careful consideration should be given to this source of overstrength when attempting to guarantee a weak column-strong beam (hereafter, WCSB) failure mechanism for the overall structure. Ignoring this effect will probably lead to premature buckling of the joist girder diagonals. The WCSB mechanism adopted here is a possible solution to obtain ductile behavior and good energy dissipation for one-story steel-framed structures subjected to strong ground motions. For this type of structure, it is easier and more reliable to obtain ductile behavior from the column than from the joist.

As shown in Figure 19, for the four column base conditions examined for the three-bay frame case, both the linear PR and fixed column base cases induce an additional force into the joist girder members. This results in a sudden failure due to the buckling of angle members of the joist girder instead of a ductile WCSB failure mechanism based on column yielding. Since SAP2000 cannot trace the frame behavior after the initial buckling of the angle members, pushover curves were truncated around 330.2 mm (13 in.) for the linear PR and 177.8 mm (7 in.) for the fixed column base cases. For this case, the design drift limit (H/100) is 91.4 mm (3.6 in.).

From these results, it can be seen that these structures are extremely flexible, and that the collapse mechanism based on column yielding does not occur until a 4% drift (366 mm or 14.4 in.) is reached. Moreover, the base shear required to reach yield (about 284 kN or 63.9 kips) is about 70% of the participating mass. This means that an extremely large

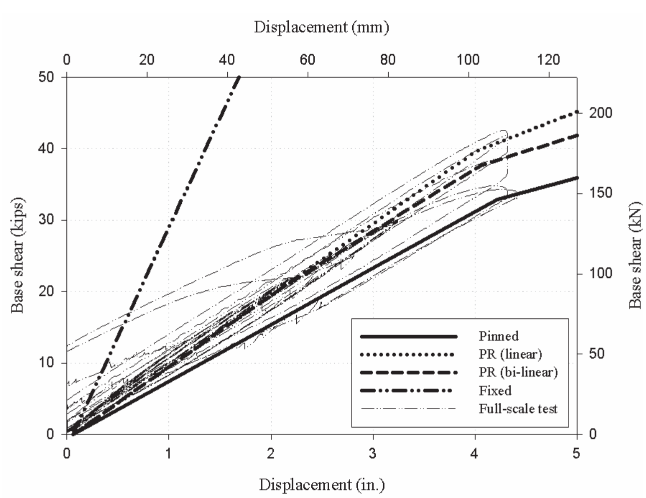

Fig. 18. Magnified pushover curves for column base fixity (one-bay frame).

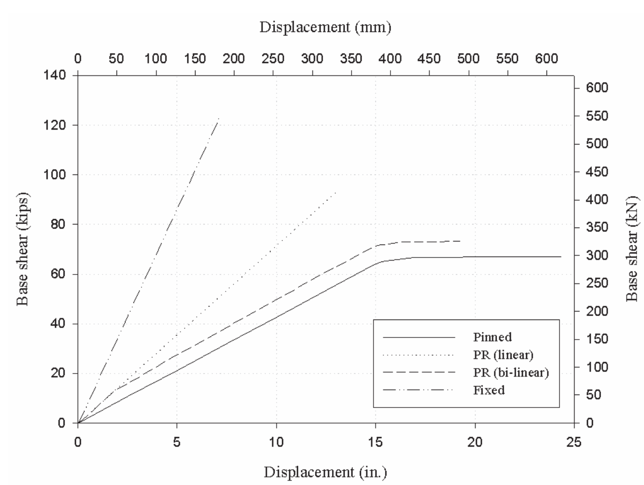

Fig. 19. Pushover curves for column base fixity (three-bay frame).

Table 5. Moment for the Column Members of the Three-Bay Frame				
Member	Location	Moment in kN-m (kip-in.)		$\lvert M_{base} / M_{top} \rvert$ for PR Base
		Pinned	Bilinear PR	
Left Exterior Column	Top	–617 (–5,464)	–604 (–5,346)	0.113
	Base	0 (0)	68 (605)	
Left Interior Column	Top	–730 (–6,458)	–713 (–6,310)	0.073
	Base	0 (0)	52 (458)	
Right Interior Column	Top	–728 (–6,444)	–712 (–6,300)	0.080
	Base	0 (0)	57 (506)	
Right Exterior Column	Top	–621 (–5,493)	–606 (–5,366)	0.079
	Base	0 (0)	48 (424)	

ground acceleration or large local soil amplification will probably be required to yield this structure. To reach a 3.5% roof drift (320 mm or 12.6 in.), the frame with linear or bilinear PR column bases requires over 67% and 13% additional force, respectively, as compared to the force required for the frame with pinned column bases (Figure 19). The results from the bilinear model are more reasonable because the bilinear model considers the column base yielding. More importantly, this means that in order to prevent an initial buckling failure of a joist girder member and maintain a WCSB mechanism, the design forces for the joist girder members and the connection need to be increased due to the additional force.

Tables 4 and 5 present the moments for the column members of the one-bay and three-bay frames, respectively. The moments induced at the column base considering the PR effects are $0.17M_{top}$ for the one-bay frame and $0.10M_{top}$ for the three-bay frame. The roof drift can be decreased by considering a PR column base but special considerations are then needed to achieve a WCSB mechanism because additional axial forces are induced into the top and bottom chord members due to the increased base shear.

CONCLUSIONS

The following conclusions can be made from this study:

1. A column base model based on the 'component model' gave good agreement with the test results (within 5%). Based on that model, simplified moment-rotation models can be developed for the column base with two anchor rods and four anchor rods.

2. The results from the bilinear model for the column base were more accurate than those from the linear model at a relatively small computation penalty.

3. The frame with PR column bases had a shorter natural period and attracts larger base shear forces. Therefore, careful consideration should be taken to incorporate this source of overstrength in design as it can result in overloading and sudden buckling of joist girder members.

4. The new suggested iterative design procedure for considering column base fixity requires two additional steps in design. First, the rotational stiffness of the column base is calculated using the component method. Second, the structural analysis is performed again with the new column base spring, and the column base is redesigned based on the induced moment from the new PR column base. Figure 20 contains a flowchart of the modified column base design procedure.

ACKNOWLEDGMENTS

This work was conducted under the sponsorship of the Steel Joist Institute. The opinions presented are solely those of the authors and not of the Steel Joist Institute or any other organization.

NOTATION

a_{eqel} = equivalent width of the T-stub [$= t_w + 2.5t_p$]

A_s = sectional area of the anchor rod

d = depth of column member

E_c = modulus of elasticity of concrete

E_s = modulus of elasticity of steel

H = height of the structure

k_b = stiffness coefficient of the rod

k_{base} = stiffness of column base

k_c = stiffness coefficient of the concrete component

k_{conn} = stiffness of the girder-to-column connection

k_p = stiffness coefficient of the plate

l_{eff} = effective length of a T-stub flange

L = length of the T-stub

L_b = length of the anchor rod shank

LVDT = linearly varying displacement transducer or linearvariable differential transformer

m = distance between web of the T-stub and the anchor rod

M_{base} = moment at the column base

M_{top} = moment at the top of the column

S_j = assembled elastic stiffness of column base

t_p = base plate thickness

t_w = column web or flange thickness

z = length of lever arm

REFERENCES

Hibbit, Karlsson, and Sorensen (1998), *ABAQUS Theory and User's Manual—Version 5.8*, Hibbit, Karlsson & Sorensen, Inc., Pawtucket, RI.

AISC (1990), *Steel Design Guide Series 1—Column Base Plates*, American Institute of Steel Construction, Inc., Chicago, IL.

AISC (2001), LRFD *Manual of Steel Construction*, 3rd Ed., American Institute of Steel Construction, Inc., Chicago, IL.

AISC (2005), *Seismic Provisions for Structural Steel Buildings Including Supplement 1*, American Institute of Steel Construction, Inc., Chicago, IL.

ASCE (2005), *Minimum Design Loads for Buildings and Other Structures*, ANSI/ASCE 7-05, American Society of Civil Engineers, Reston, VA.

Beckman, M.W. (1996), "Seismic Analysis and Design of Multi-Bay Rigid Trussed Frames," MS Thesis, Department of Civil Engineering, University of Minnesota, Minneapolis, MN.

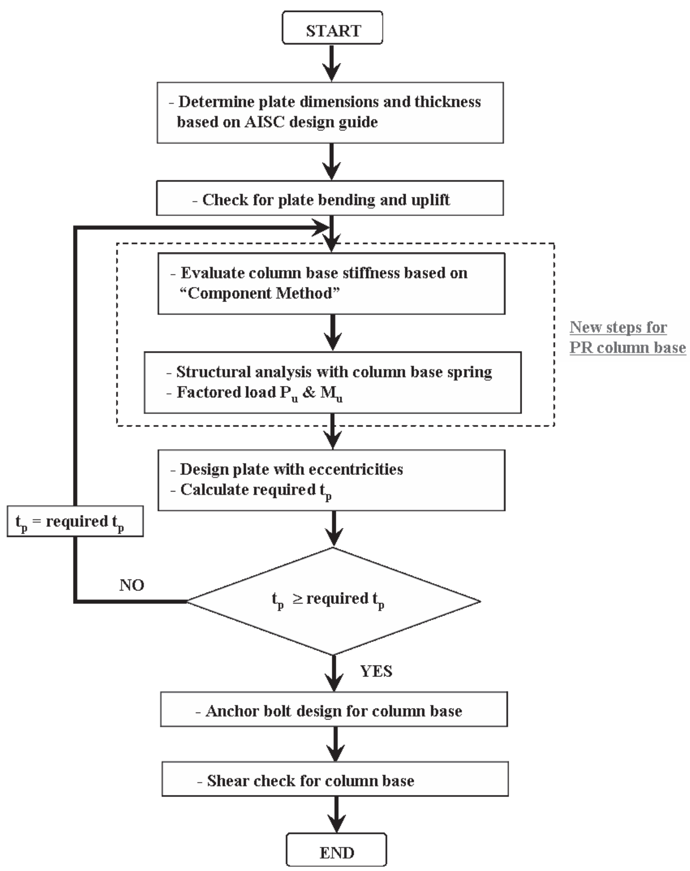

Fig. 20. Flowchart for proposed column base design procedure.

CEN (1998), *Eurocode 3—Revised Annex J: Joints in Building Frames*, Document ENV 1993-1-1:1992/A2, Brussels.

European Commission (1999), COST C1, *Column Bases in Steel Building Frames*, Brussels.

ICC (2000), *International Building Code*, International Code Council, Falls Church, VA.

Kim, U.S. (2003), "Seismic Behavior of Steel Joist Girder Structures," Ph.D. Dissertation, School of Civil and Environmental Engineering, Georgia Institute of Technology, Atlanta, GA.

Kim, U.S., Leon, R.T., and Galambos, T.V. (2007), "Seismic Design of Steel Joist Girder Structures," *Engineering Journal*, AISC, Vol. 44, No. 3, pp. 233–242.

Leon, R.T., Kim, U.S., and Galambos, T.V. (2003), "Seismic Design of Trussed Girder Systems," Keynote Presentation, ASSCCA '03, Sydney, Australia.

Leon, R.T. (1994), "Composite Semi-Rigid Construction," *Engineering Journal*, AISC, Vol. 31, No. 2, pp. 57–67.

Mathsoft (2000), *MathCad 2000 Professional*, Mathsoft, Inc., Cambridge, MA.

OSHA (2001), *Safety Standards for Steel Erection: Final Rule*, 29 CFR Part 1296.

Picard, A. and Beaulieu, D. (1985), "Behavior of a Simple Column Base Connection," *Canadian Journal of Civil Engineering*, Vol. 12, pp. 126–136.

Picard, A., Beaulieu, D., and Pérusse, B. (1987), "Rotational Restraint of a Simple Column Base Connection," *Canadian Journal of Civil Engineering*, Vol. 14, pp. 49–57.

SAC (1997), "Protocol for Fabrication, Inspection, Testing, and Documentation of Beam-Column Connection Tests and Other Experimental Specimens," SAC/BC-97/02, SAC Joint Venture, Sacramento, CA.

Computers and Structures (1998), *SAP2000 Tutorial Manuals—Version 7.0*, Computers and Structures, Inc., Berkeley, CA.

SJI (2002), *41st Edition Standard Specifications—Load Tables and Weight Tables for Steel Joists and Joist Girders*, Steel Joist Institute, Myrtle Beach, SC.

Stojadinović, B., Spacone, E., Goel, S.C., and Kwon, M. (1998), "Influence of Semi-Rigid Column Base Models on the Response of Steel MRF Buildings," *Proceedings,* 6th U.S. National Conference on Earthquake Engineering, Seattle, WA.

Thornton, W.A. (1990), "Design of Base Plates for Wide Flange Columns—A Concatenation of Methods," *Engineering Journal*, AISC, Vol. 27, No. 4, pp. 173–174.

Wald, F. and Jaspart, J.P. (1998), "Stiffness Design of Column Bases," *Journal of Constructional Steel Research*, Vol. 46, 1-3, Paper No. 135.